Voltage Multiplier based Non-Isolated Buck-Boost Converter

Yasser Almalaq
Electrical Engineering Department, University of Ha'il, Saudi Arabia
ya.almalaq@uoh.edu.sa (corresponding author)

Ayoob Alateeq
Electrical Engineering Department, University of Ha'il, Saudi Arabia
a.alateeq@uoh.edu.sa

Abdulaziz Alateeq
Electrical Engineering Department, University of Ha'il, Saudi Arabia
Aj.alateeq@uoh.edu.sa

Received: 3 October 2023 | Revised: 16 October 2023 | Accepted: 20 October 2023

Licensed under a CC-BY 4.0 license | Copyright (c) by the authors | DOI: https://doi.org/10.48084/etasr.6466

ABSTRACT

This paper presents a new non-isolated high-gain Buck-Boost Converter (BBC) that uses a switched-inductor (SL) voltage multiplier. This type of DC-DC converter can be very useful in renewable energy applications, especially PV, where the output DC voltage is stepped up to a higher voltage. The output voltage of the proposed switched-inductor BBC (SLBBC) is around 15 times the input voltage with positive polarity when a 0.75 duty cycle of the power switches is used. This is achieved without the use of a transformer or common-core coupled inductors, so the topology is simple to construct. This high output voltage is achieved by using the SL voltage multiplier, which consists of three diodes and two inductors. There are two power switches that operate synchronously, which is an advantage of the design. However, it is discovered that the voltage gain in the step-down mode of the proposed converter is less than that of the other converters. The proposed converter is analyzed in the Continuous Conduction Mode (CCM). The operating principles and steady-state analysis are presented in detail. MATLAB/Simulink was used to prove the effectiveness of the proposed SLBBC.

Keywords-buck-boost converter; Continuous Conduction Mode (CCM); DC-DC converter; photovoltaic; switched-inductor (SL)

I. INTRODUCTION

Photovoltaic (PV) panels are unsuitable for AC grid integration due to their low output voltage. Therefore, a series connection of PV arrays is required to achieve a large DC voltage. However, this is challenging due to the shadow effect in PV panels [1]. Non-isolated DC-DC converters with a high voltage gain in the step-up or step-down mode that can change the input voltage to a higher or lower value are required in a variety of applications, such as PV applications, fuel cell systems, storage batteries, car electronic devices, and many others [2]. Although buck and boost converters have simple structure and high efficiency, they are not suitable for low or high output voltage due to the limitation on the voltage gain [3]. It is common knowledge that the topology of a switching mode power supply is the most important factor in determining how effectively the system will function and how components should be selected [4]. As a result, this topic has received much attention in research, and over the past few decades, various buck-boost topologies have been suggested. The simplest topology of BBC is the conventional BBC (see Figure 1), which is a DC-DC converter that has an output voltage magnitude that is larger or smaller than the input voltage with polarity inverted, as can be obviously seen from its voltage conversion ratio (see (1)). The value of the duty cycle (D) determines if the BBC is in the step-up mode or step-down mode. If D is less than 0.5, the BBC will function as a buck converter and as a boost converter when D is greater than 0.5. In step-up mode, the BBC has limited voltage gain and therefore cannot maintain a high output voltage. Although high voltage gain can be achieved at extreme duty cycles (lower than 0.1 in step-down or more than 0.9 in step-up), it is difficult due to the practical constraints of power semiconductor devices. Although the BBC has other forms, such as the Cuk converter, Zeta converter, and Single-Ended Primary Inductor Converter (SEPIC), they all have the same limited voltage gain [5]. However, the Cuk converter has many advantages. It has continuous input and output current and negative output voltage, which can be suitable for applications such as audio amplifiers and signal generators [6].

$$M = \frac{V_{out}}{V_{in}} = -\frac{D}{1-D} \quad (1)$$

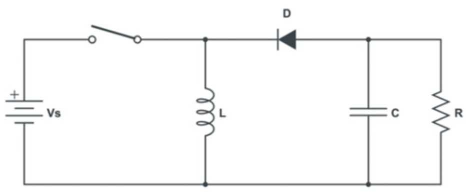

Fig. 1. Conventional buck-boost converter.

Various wide voltage gain converters with winding-cross-coupled inductors are represented in [7]. However, the switches suffer from high voltage spikes, and the system has low efficiency due to the expected leakage in the winding-cross-coupled inductors. This is why the coupled inductor technique is not used in the proposed topology. A novel single-switch cascaded BBC is represented in [8]. However, the output voltage is floating. A modified topology of the conventional BBC is presented in [9], but the output is inverted. A new buck-boost topology is presented in [10], with a low voltage stress. However, the proposed converter has high ripples, and the voltage gain is limited. Quadratic converters, which are represented in [11, 12], can accomplish high voltage gain, but their efficiency is low. A semi-quadratic BBC is presented in [13]. However, the input current is discontinuous, and there is no common ground. The Luo converter using the voltage lift technique is presented in [14, 15]. Although a high voltage gain can be achieved, this kind of topology is complex, expensive, and inefficient. Another topology is the interleaved converter, which is presented in [16-18]. Although this converter can obtain high voltage gain with low voltage stress across switches, this topology faces complexity in its operating mode, converter structure, and control strategy. Other techniques of designing high gain converters are presented in [19-21].

A non-isolated high-gain DC-DC switched-inductor buck-boost converter (SLBBC) with a simple structure is presented in this paper. This type of DC-DC converter can be very useful in renewable energy applications, especially PVs. The output voltage of the proposed SLBBC is 15 times the input voltage with positive polarity when a 0.75 duty cycle of the power switches is used. The SL technique is used in a modified BBC, where three inductors are magnetized when switches are turned on, and three inductors are demagnetized when switches are turned off.

II. PROPOSED TOPOLOGY STRUCTURE, OPERATING PRINCIPLE, AND ANALYSIS

A. Power Circuit

The configuration of the proposed SLBBC is shown in Figure 2. Its main power stage involves two power switches (Q_1 and Q_2), five diodes (D_1, D_2, D_3, D_4, and D_5), three inductors (L_1, L_2, and L_3), two capacitors (C_1 and C_2), and one resistive load (R_1). The two power switches (Q_1 and Q_2) are the only two parts to be controlled, and they work instantaneously. In the proposed converter, the currents passing through L_1, L_2, L_3, C_1, C_2, Q_1, Q_2, D_1, D_2, D_3, D_4, and D_5 are defined as i_{L1}, i_{L2}, i_{L3}, i_{C1}, i_{C2}, i_{O1}, i_{O2}, i_{D1}, i_{D2}, i_{D3}, i_{D4}, and i_{D5}, respectively. The respective voltages are v_{L1}, v_{L2}, v_{L3}, v_{C1}, v_{C2}, v_{O1}, v_{O2}, v_{D1}, v_{D2}, v_{D3}, v_{D4}, and v_{D5}. The output is connected to a resistive load R_1 whose current and voltage is denoted as i_{out} and v_{out}. Note that $v_{C2} = v_{out}$. The input current and voltage are i_{in} and v_{in} where $i_{in} = i_{O1}$. The duty cycle (D) is applied to the switches Q_1 and Q_2. I_{in}, V_{in}, I_{out}, and V_{out} are assumed to be the DC values in steady state of i_{in}, v_{in}, i_{out}, and v_{out}. T_S is the switching period which is equal to $1/f_S$, where f_S is the switching frequency. Figure 3 shows the time domain waveform of the proposed SLBBC operating in CCM.

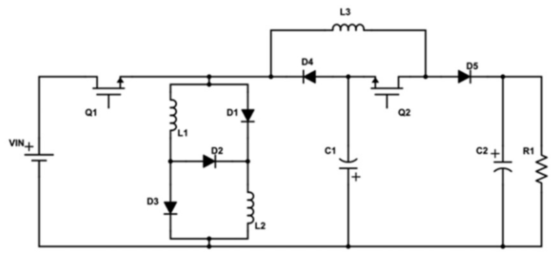

Fig. 2. The proposed SLBBC.

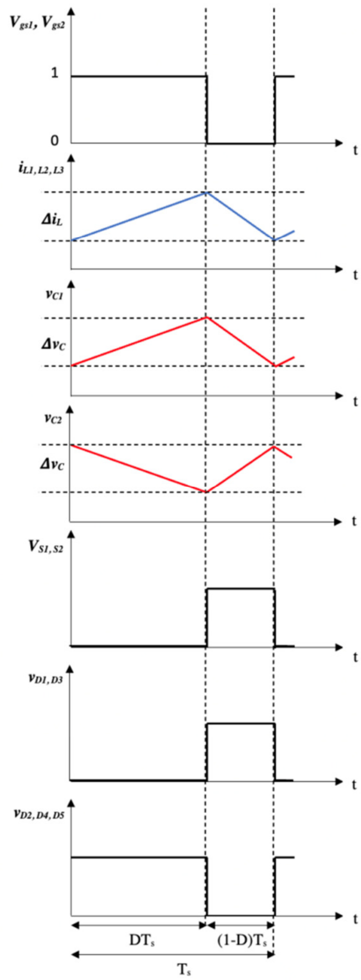

Fig. 3. Main steady-state waveforms of the proposed SLBBC.

B. Modes of Operation

Mode 1: In this time interval, as shown in Figure 4, switches Q_1 and Q_2 are turned on, power diodes D_1 and D_3 are forward biased, and power diodes D_2, D_4, and D_5 are reversed biased. The voltage source V_{in} magnetizes inductors L_1, L_2, and L_3 and charges C_1 through switches Q_1 and Q_2.

Mode 2: In this time interval, as shown in Figure 5, switches Q_1 and Q_2 are turned off, power diodes D_2, D_4, and D_5 are forward biased, and power diodes D_1 and D_3 are reversed biased. It is obviously seen from Figure 5 that the energy stored in L_1 and L_2 is demagnetized to charge capacitor C_1 via D_2 and D_4. At the same time, the energy stored in inductor L_3 is demagnetized to charge capacitors C_1 and C_2 and the resistive load R_l via the diodes D_4 and D_5.

C. Circuit Analysis

Steady-state analysis is performed based on the following assumptions to analyze the proposed SLBBC:

- All the components used including power switches, diodes, inductors, capacitors, and resistors are ideal.
- The two capacitors C_1 and C_2 are sufficiently large enough so that the voltages across them are considered as constant.

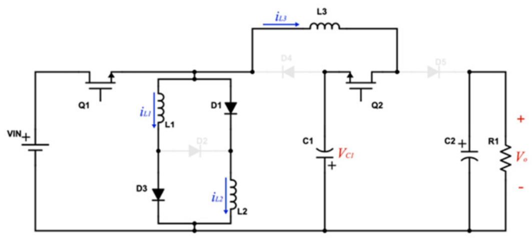

Fig. 4. The proposed SLBBC in the ON mode.

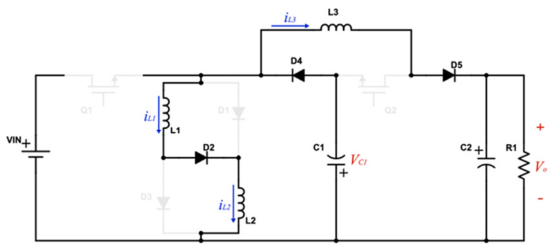

Fig. 5. Proposed SLBBC in the OFF mode.

- The natural time constant of the converter is much higher than the switching period T_S.
- Only the CCM of the proposed BBC is investigated, which is the status when the current passing through the inductors flows continuously. On the other hand, the interval when the inductor current remains zero is the Discontinuous Conduction Mode (DCM). Increased stresses on semiconductor switches, increased rating of passive components, noise, and electromagnetic interference (EMI) are all disadvantages of using DCM [25].

When the two MOSFETs are turned on, the voltages across the inductors L_1, L_2, and L_3 are expressed as:

$$V_{L_1} = V_{L_2} = V_{in} \quad (2)$$

$$V_{L_3} = V_{in} + V_{C_1} \quad (3)$$

When the two MOSFETs are turned off, the voltages across the inductors are expressed as:

$$V_{L_1} = V_{L_2} = -\frac{V_{C_1}}{2} \quad (4)$$

$$V_{L_3} = -\left(V_{C_1} + V_{C_2}\right) \quad (5)$$

By applying the volt second method to the inductors, the following expressions can be obtained:

$$V_{in}D - \frac{V_{C_1}}{2}(1-D) = 0 \quad (6)$$

$$\left(V_{in} + V_{C_1}\right)D - \left(V_{C_1} + V_{out}\right)(1-D) = 0 \quad (7)$$

From (6), the expression of the voltage across the capacitor C_1 can be obtained as in (8):

$$V_{C_1} = -\frac{2D}{1-D}V_{in} \quad (8)$$

By substituting (8) into (7), the ideal voltage gain of the proposed converter can be obtained:

$$M = \frac{V_{out}}{V_{in}} = \frac{D(3D-1)}{(1-D)^2} \quad (9)$$

D. Voltage Stress

The amount of voltage stress across C_1 is calculated by:

$$V_{C_1} = -\frac{2D}{1-D}V_{in} = -\frac{2(1-D)}{3D-1}V_{out} \quad (10)$$

Also, the voltage stress across the two power switches and the five diodes can be derived by:

$$V_{Q_1} = \frac{1+D}{1-D}V_{in} = \frac{1+D^2}{D(3D-1)}V_{out} \quad (11)$$

$$V_{Q_2} = \frac{1+D}{(1-D)^2}V_{in} = \frac{1+D}{D(3D-1)}V_{out} \quad (12)$$

$$V_{D_1} = V_{D_3} = \frac{D}{1-D}V_{in} = \frac{1-D}{3D-1}V_{out} \quad (13)$$

$$V_{D_2} = V_{in} = \frac{(1-D)^2}{D(3D-1)}V_{out} \quad (14)$$

$$V_{D_4} = \frac{1+D}{1-D}V_{in} = \frac{1+D^2}{D(3D-1)}V_{out} \quad (15)$$

$$V_{D_5} = \frac{D(1+D)}{(1-D)^2}V_{in} = \frac{1+D}{3D-1}V_{out} \quad (16)$$

E. Current Stress

Assuming the circuit is ideal, (17) and (18) are obtained:

$$P_{in} = P_{out} \quad (17)$$

$$V_{in}I_{in} = V_{out}I_{out} \quad (18)$$

The relationship between the DC input current and the output current is obtained in (19) according to the voltage gain obtained in (9).

$$\frac{I_{out}}{I_{in}} = \frac{(1-D)^2}{D(3D-1)} \quad (19)$$

The Ohm's law for the resistive load R_1 is shown in (20):

$$V_{out} = R_1 I_{out} \quad (20)$$

From the Volt second method, I_{in} and I_{out} can be obtained as functions of I_{L1}, I_{L2}, and I_{L3}. Note that $I_{L1} = I_{L2} = I_{Lin}$.

$$I_{in} = D\left(I_{L_1} + I_{L_2} + I_{L_3}\right) = D\left(2I_{L_{in}} + I_{L_3}\right) \quad (21)$$

$$I_{out} = (1-D)I_{L_3} \quad (22)$$

From (9) and (18)-(22), the currents I_{L1}, I_{L2}, and I_{L3} can be obtained:

$$I_{L_{in}} = I_{L_1} = I_{L_2} = \frac{D(2D-1)(3D-1)}{(1-D)^4 R_1} V_{in} \quad (23)$$

$$I_{L_3} = \frac{D(3D-1)}{(1-D)^3 R_1} V_{in} \quad (24)$$

The currents of the two power switches and the five diodes can be derived from the voltage stress:

$$I_{Q_1} = D\left(I_{L_1} + I_{L_2} + I_{L_3}\right) = \frac{D^2(9D^2-6D+1)}{(1-D)^4 R_1} V_{in} \quad (25)$$

$$I_{Q_2} = D I_{L_3} = \frac{D^2(3D-1)}{(1-D)^3 R_1} V_{in} \quad (26)$$

$$I_{D_1} = I_{D_3} = D I_{L_{in}} = \frac{D^2(2D-1)(3D-1)}{(1-D)^4 R_1} V_{in} \quad (27)$$

$$I_{D_2} = (1-D) I_{L_{in}} = \frac{D(2D-1)(3D-1)}{(1-D)^3 R_1} V_{in} \quad (28)$$

$$I_{D_4} = (1-D)\left(I_{L_{in}} + I_{L_3}\right) = \frac{D^2(3D-1)}{(1-D)^3 R_1} V_{in} \quad (29)$$

$$I_{D_5} = (1-D) I_{L_3} = \frac{D(3D-1)}{(1-D)^2 R_1} V_{in} \quad (30)$$

Table I summarizes the voltage stresses and current stresses for all the parameters of the proposed SLBBC.

TABLE I. VOLTAGE AND CURRENT STRESSES OF THE PROPOSED SLBBC

Parameter	Voltage Stress	Current Stress
L_1, L_2	-	$\frac{D(2D-1)(3D-1)}{(1-D)^4 R_1} V_{in}$
L_3	-	$\frac{D(3D-1)}{(1-D)^3 R_1} V_{in}$
C_1	$-\frac{2D}{1-D} V_{in}$	-
C_2	$\frac{D(3D-1)}{(1-D)^2} V_{in}$	-
Q_1	$\frac{1+D}{1-D} V_{in}$	$\frac{D^2(9D^2-6D+1)}{(1-D)^4 R_1} V_{in}$
Q_2	$\frac{1+D}{(1-D)^2} V_{in}$	$\frac{D^2(3D-1)}{(1-D)^3 R_1} V_{in}$
D_1, D_3	$\frac{D}{1-D} V_{in}$	$\frac{D^2(2D-1)(3D-1)}{(1-D)^4 R_1} V_{in}$
D_2	V_{in}	$\frac{D(2D-1)(3D-1)}{(1-D)^3 R_1} V_{in}$
D_4	$\frac{1+D}{1-D} V_{in}$	$\frac{D^2(3D-1)}{(1-D)^3 R_1} V_{in}$
D_5	$\frac{D(1+D)}{(1-D)^2} V_{in}$	$\frac{D(3D-1)}{(1-D)^2 R_1} V_{in}$

F. Current Ripples of Inductors

The ripples of the inductors' currents i_{L1}, i_{L2}, and i_{L3} can be obtained by:

$$\Delta i_{L_1} = \frac{V_{L_1}}{L_1} D T_S = \frac{D}{L_1 f_S} V_{in} \quad (31)$$

$$\Delta i_{L_2} = \frac{V_{L_2}}{L_2} D T_S = \frac{D}{L_2 f_S} V_{in} \quad (32)$$

$$\Delta i_{L_3} = \frac{V_{L_3}}{L_3} D T_S = \frac{D(1+D)}{L_3 f_S} V_{in} \quad (33)$$

By knowing the inductors' current ripples, the input voltage V_{in}, the duty cycle D, and the switching frequency f_S, the appropriate values of inductors L_1, L_2, and L_3 can be calculated using (31), (32), and (33).

G. Voltage Ripples of Capacitors

The ripples of the capacitors' voltages v_{C1} and v_{C2} across capacitors C_1 and C_2 are obtained by:

$$\Delta v_{C_1} = \frac{\Delta Q}{C_1} = \frac{(3D-1)}{2(1-D)R_1 C_1 f_S} V_{out} \quad (34)$$

$$\Delta v_{C_2} = \frac{\Delta Q}{C_2} = \frac{D}{R_1 C_2 f_S} V_{out} \quad (35)$$

By knowing the capacitors' voltage ripples, the output voltage V_{out}, the duty cycle D, and the switching frequency f_S, the appropriate values of capacitors C_1 and C_2 can be calculated by (34) and (35).

III. COMPARISON ANALYSIS

The main reason for designing the proposed SLBBC is its ability to achieve a high voltage gain in step-up mode compared with other BBCs, as shown in Figure 6. The high voltage gain is obtained without a transformer or coupling inductors, which would increase the converter's size, losses, and overall cost. Figure 7 shows a comparison between the single switch buck-boost, hybrid buck-boost, KY buck-boost, and proposed SLBBC in terms of number of switches, diodes, inductors, and capacitors used in each converter.

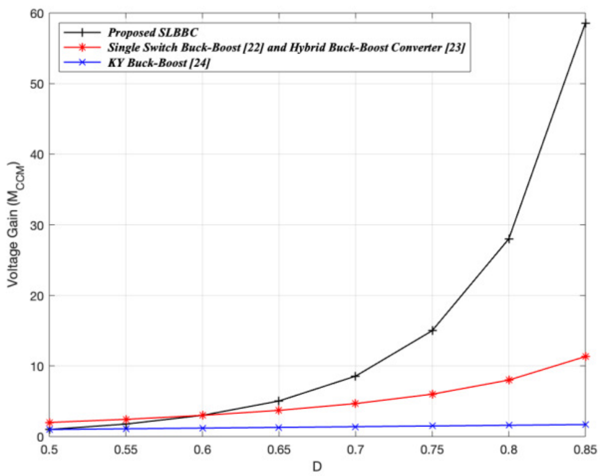

Fig. 6. Voltage gain comparison.

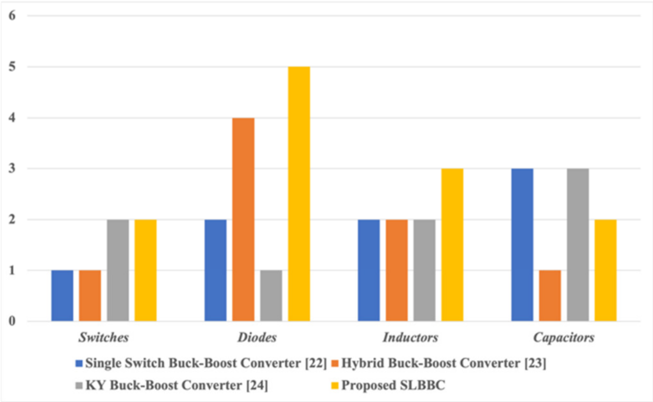

Fig. 7. Comparison of the number of switches, diodes, inductors, and capacitors.

IV. RESULTS AND DISCUSSION

The proposed SLBBC was designed in the MATLAB/Simulink for 12 V input voltage, 200 W rated power, 50 kHz switching frequency, and 0.65 duty cycle as shown in Figure 8. The duty cycle is greater than 0.5, therefore, the proposed converter operates in step-up mode. The proposed converter's specifications are shown in Table II. The switches Q_1 and Q_2 will operate simultaneously, and their gate pulses are shown in Figures 9 and 10. The waveforms of the currents passing through the three inductors are shown in Figure 9. The three inductors will be magnetized when the two switches are turned on, and they will be demagnetized when the two switches are turned off. By using the current stress equations (23) and (24) passing through L_1, L_2, and L_3, the theoretical values of currents are around 9 A and 11 A. Figure 10 depicts the voltage waveform across C_1. The capacitor C_1 will charge when the two switches are turned on, and it will discharge when they are turned off. By using the voltage stress equation (10) on C_1, the theoretical value of the voltage is -44 V. Figure 10 shows the voltage across the charge pump capacitor C_2. As shown in Figures 4 and 5, C_2 discharges when the two switches are turned on, and charges when they are turned off. By using the voltage gain formula (9), the theoretical output voltage on the load R_l and the charge pump capacitor C_2 is around 60 V. Figure 11 shows the input voltage V_{in}, which is 12 V, the output voltage V_{out}, which is around 60 V, and the output power P_{out}, which is 200 W. The efficiency curve as a function of P_{out} is shown in Figure 12. A peak efficiency of 93.14% is achieved when the output power is 340 W. From the above comparisons between the theoretical and the simulation results, one can see that they are in accordance, proving the correctness of the theoretical analysis.

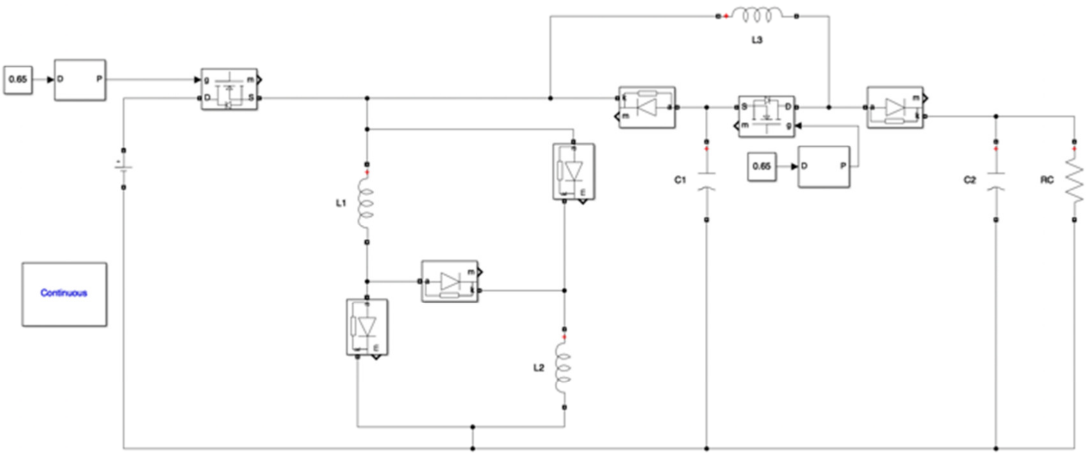

Fig. 8. Simulink model of the SLBBC.

TABLE II. COMPONENTS SPECIFICATIONS

Parameter	Value	Unit
Input voltage (V_{in})	12	V
Output voltage (V_{out})	57	V
Rated power (P_{out})	200	W
Switching frequency (f_S)	50	kHz
Duty cycle (D)	0.65	-
Inductors (L_1, L_2, and L_3)	3	mH
Capacitor (C_1)	20	μF
Capacitor (C_2)	100	μF
Load (R_l)	15	Ω

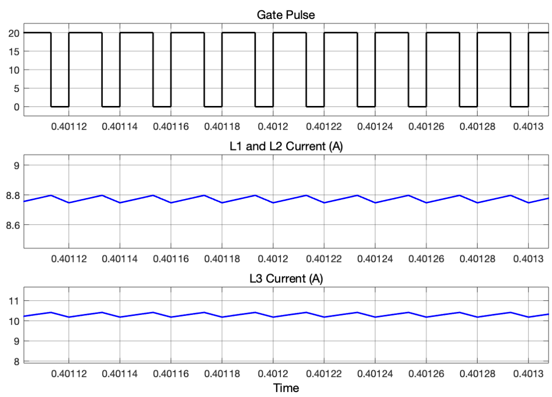

Fig. 9. Current waveforms of L_1, L_2, and L_3.

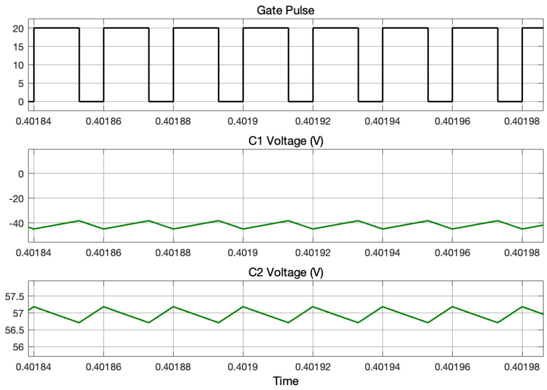

Fig. 10. Voltage waveforms of C_1 and C_2.

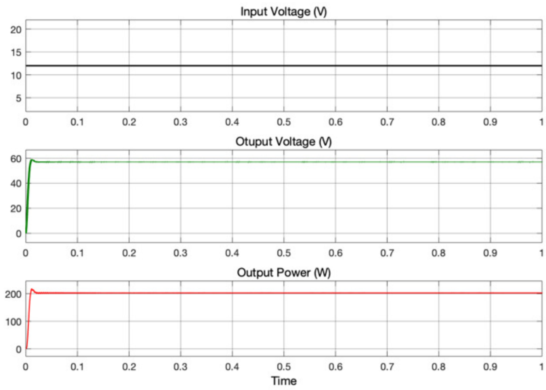

Fig. 11. Waveforms of V_{in}, V_{out}, and P_{out}.

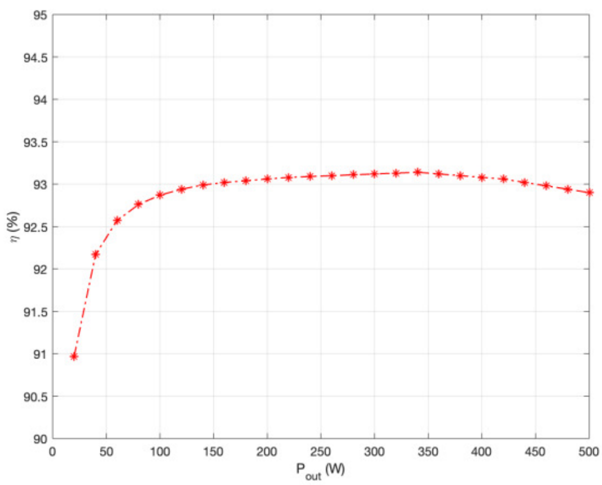

Fig. 12. Efficiency curve as function of P_{out}.

V. CONCLUSION

In this paper, a new SLBBC is proposed to make up for the fact that the traditional buck-boost converter has a low voltage gain. The proposed converter can achieve high step-up voltage gain by using the SL technique, which is useful in PV and industrial applications requiring high step-up or step-down voltage gain. The SL voltage multiplier, which consists of two inductors and three diodes, is placed in the buck-boost converter instead of a single inductor. The two inductors will charge during the ON mode, and they will discharge during the OFF mode. The advantages of the proposed converter are its ability to maintain high step-up voltage gain, its simple construction, and a positive output voltage. Details such as the operating principles, steady-state analysis, and a comparison to other buck-boost converters are provided. The results of the theoretical analysis and the MATLAB/Simulink simulation were matched, which showed that the output could have a high voltage gain.

ACKNOWLEDGMENT

The authors like to acknowledge the help and thank the Deanship of Scientific Research at the University of Ha'il for funding this research paper (project number BA-2131).

REFERENCES

[1] A. E. Khosroshahi, A. Mohammadpour Shotorbani, H. Dadashzadeh, A. Farakhor, and L. Wang, "A New Coupled Inductor-Based High Step-Up DC-DC Converter for PV Applications," in *2019 20th Workshop on Control and Modeling for Power Electronics (COMPEL)*, Toronto, ON, Canada, Jun. 2019, https://doi.org/10.1109/COMPEL.2019.8769630.

[2] S. Miao, F. Wang, and X. Ma, "A New Transformerless Buck–Boost Converter With Positive Output Voltage," *IEEE Transactions on Industrial Electronics*, vol. 63, no. 5, pp. 2965–2975, Feb. 2016, https://doi.org/10.1109/TIE.2016.2518118.

[3] T.-F. Wu and Y.-K. Chen, "Modeling PWM DC/DC converters out of basic converter units," *IEEE Transactions on Power Electronics*, vol. 13, no. 5, pp. 870–881, Sep. 1998, https://doi.org/10.1109/63.712294.

[4] J. Li and J. Liu, "A Novel Buck–Boost Converter With Low Electric Stress on Components," *IEEE Transactions on Industrial Electronics*, vol. 66, no. 4, pp. 2703–2713, Apr. 2019, https://doi.org/10.1109/TIE.2018.2847646.

[5] H. Shayeghi, S. Pourjafar, and F. Sedaghati, "Presented a transformer-less buck-boost DC–DC structure with vast voltage range," *IET Power Electronics*, vol. 15, no. 7, pp. 659–674, 2022, https://doi.org/10.1049/pel2.12257.

[6] M. R. Banaei and S. G. Sani, "Analysis and Implementation of a New SEPIC-Based Single-Switch Buck–Boost DC–DC Converter With Continuous Input Current," *IEEE Transactions on Power Electronics*, vol. 33, no. 12, pp. 10317–10325, Sep. 2018, https://doi.org/10.1109/TPEL.2018.2799876.

[7] W. Li and X. He, "A Family of Interleaved DC–DC Converters DeducedFrom a Basic Cell With Winding-Cross-CoupledInductors (WCCIs) for High Step-Upor Step-Down Conversions," *IEEE Transactions on Power Electronics*, vol. 23, no. 4, pp. 1791–1801, Jul. 2008, https://doi.org/10.1109/TPEL.2008.925204.

[8] J. Fu, B. Zhang, D. Qiu, and W. Xiao, "A novel single-switch cascaded DC-DC converter of Boost and Buck-boost converters," in *2014 16th European Conference on Power Electronics and Applications*, Lappeenranta, Finland, Dec. 2014, pp. 1–9, https://doi.org/10.1109/EPE.2014.6910723.

[9] M. R. Banaei and H. A. F. Bonab, "A Novel Structure for Single-Switch Nonisolated Transformerless Buck–Boost DC–DC Converter," *IEEE Transactions on Industrial Electronics*, vol. 64, no. 1, pp. 198–205, Jan. 2017, https://doi.org/10.1109/TIE.2016.2608321.

[10] H.-S. Son, J.-K. Kim, J.-B. Lee, S.-S. Moon, J.-H. Park, and S.-H. Lee, "A New Buck–Boost Converter With Low-Voltage Stress and Reduced Conducting Components," *IEEE Transactions on Industrial Electronics*, vol. 64, no. 9, pp. 7030–7038, Sep. 2017, https://doi.org/10.1109/TIE.2017.2686300.

[11] J. A. Morales-Saldaña, R. Loera-Palomo, E. Palacios-Hernández, and J. L. González-Martínez, "Modelling and control of a DC–DC quadratic boost converter with R2P2," *IET Power Electronics*, vol. 7, no. 1, pp. 11–22, 2014, https://doi.org/10.1049/iet-pel.2012.0749.

[12] J. C. Mayo-Maldonado, J. E. Valdez-Resendiz, P. M. Garcia-Vite, J. C. Rosas-Caro, M. del Rosario Rivera-Espinosa, and A. Valderrabano-Gonzalez, "Quadratic Buck–Boost Converter With Zero Output Voltage Ripple at a Selectable Operating Point," *IEEE Transactions on Industry Applications*, vol. 55, no. 3, pp. 2813–2822, Feb. 2019, https://doi.org/10.1109/TIA.2018.2889421.

[13] L. Nousiainen and T. Suntio, "Dynamic characteristics of current-fed semi-quadratic buck-boost converter in photovoltaic applications," in *2011 IEEE Energy Conversion Congress and Exposition*, Phoenix, AZ, USA, Sep. 2011, pp. 1031–1038, https://doi.org/10.1109/ECCE.2011.6063886.

[14] F. L. Luo, "Six self-lift DC-DC converters, voltage lift technique," *IEEE Transactions on Industrial Electronics*, vol. 48, no. 6, pp. 1268–1272, Sep. 2001, https://doi.org/10.1109/41.969408.

[15] Y. He and F. L. Luo, "Analysis of Luo converters with voltage-lift circuit," *IEE Proceedings - Electric Power Applications*, vol. 152, no. 5, pp. 1239–1252, Sep. 2005, https://doi.org/10.1049/ip-epa:20045176.

[16] Y.-T. Chen, W.-C. Lin, and R.-H. Liang, "An interleaved high step-up DC-DC converter with double boost paths," *International Journal of Circuit Theory and Applications*, vol. 43, no. 8, pp. 967–983, 2015, https://doi.org/10.1002/cta.1986.

[17] L. Zhou, B. Zhu, Q. Luo, and S. Chen, "Interleaved non-isolated high step-up DC/DC converter based on the diode–capacitor multiplier," *IET Power Electronics*, vol. 7, no. 2, pp. 390–397, 2014, https://doi.org/10.1049/iet-pel.2013.0124.

[18] C.-T. Pan, C.-F. Chuang, and C.-C. Chu, "A Novel Transformerless Interleaved High Step-Down Conversion Ratio DC–DC Converter With Low Switch Voltage Stress," *IEEE Transactions on Industrial Electronics*, vol. 61, no. 10, pp. 5290–5299, Jul. 2014, https://doi.org/10.1109/TIE.2014.2301774.

[19] A. Al-Ateeq and A. J. Alateeq, "Soft-Charging Effects on a High Gain DC-to-DC Step-up Converter with PSC Voltage Multipliers," *Engineering, Technology & Applied Science Research*, vol. 10, no. 5, pp. 6323–6329, Oct. 2020, https://doi.org/10.48084/etasr.3773.

[20] Y. Almalaq and M. Matin, "Two-Switch High Gain Non-Isolated Cuk Converter," *Engineering, Technology & Applied Science Research*, vol. 10, no. 5, pp. 6362–6367, Oct. 2020, https://doi.org/10.48084/etasr.3826.

[21] V. Gopan. K. and J. D. Shree, "Implementation of a High Power Quality BLDC Motor Drive Using Bridgeless DC to DC Converter with Fuzzy Logic Controller," *Engineering, Technology & Applied Science Research*, vol. 12, no. 5, pp. 9178–9185, Oct. 2022, https://doi.org/10.48084/etasr.5213.

[22] M. R. Banaei, H. Ardi, and A. Farakhor, "Analysis and implementation of a new single-switch buck–boost DC/DC converter," *IET Power Electronics*, vol. 7, no. 7, pp. 1906–1914, 2014, https://doi.org/10.1049/iet-pel.2013.0762.

[23] B. Axelrod, Y. Berkovich, and A. Ioinovici, "Switched-Capacitor/Switched-Inductor Structures for Getting Transformerless Hybrid DC–DC PWM Converters," *IEEE Transactions on Circuits and Systems I: Regular Papers*, vol. 55, no. 2, pp. 687–696, Mar. 2008, https://doi.org/10.1109/TCSI.2008.916403.

[24] K. I. Hwu and T. J. Peng, "A Novel Buck–Boost Converter Combining KY and Buck Converters," *IEEE Transactions on Power Electronics*, vol. 27, no. 5, pp. 2236–2241, Feb. 2012, https://doi.org/10.1109/TPEL.2011.2182208.

[25] N. Mohan, *Power Electronics: A First Course*, 1st edition. Hoboken, N.J, USA: Wiley, 2011.